

# Stability diagrams for bursting neurons modeled by three-variable maps

M. Copelli<sup>a,\*</sup>, M. H. R. Tragtenberg<sup>b</sup>, O. Kinouchi<sup>c</sup>

<sup>a</sup> *Laboratório de Física Teórica e Computacional  
Departamento de Física, Universidade Federal de Pernambuco  
50670-901 Recife, PE, Brazil*

<sup>b</sup> *Departamento de Física, Universidade Federal de Santa Catarina  
88040-900 Florianópolis, SC, Brazil*

<sup>c</sup> *Departamento de Física e Matemática,  
Faculdade de Filosofia, Ciências e Letras de Ribeirão Preto,  
Universidade de São Paulo  
Av. dos Bandeirantes 3900, 14040-901 Ribeirão Preto, SP, Brazil*

---

## Abstract

We study a simple map as a minimal model of excitable cells. The map has two fast variables which mimic the behavior of class I neurons, undergoing a sub-critical Hopf bifurcation. Adding a third slow variable allows the system to present bursts and other interesting biological behaviors. Bifurcation lines which locate the excitability region are obtained for different planes in parameter space.

*Key words:* Neuron models, Coupled map lattices, Computational Neuroscience, Hindmarsh-Rose, FitzHugh-Nagumo

*PACS:* 1.3806, 3.1415

---

## 1 Introduction

Maps are dynamical systems with continuous state variables but discrete-time dynamics. They constitute low computational cost elements for large scale simulations of complex systems [1, 2, 3]. The proper use of coupled map lattices (CML) in neural modeling depends on the choice of a good basic element. Two-variable maps have been proposed by Aihara et. al. [1], Chialvo [4], and

---

\* Corresponding author

*Email address:* mcopelli@df.ufpe.br (M. Copelli).

Kinouchi and Tragtenberg [5]. Methodological considerations about the use of maps in computational neuroscience can be found in these references.

A three-variable map with one slow and two fast variables has been recently introduced by Kuva et al. [6]. It is able to reproduce complex biological behaviors, such as bursting, cardiac-like spikes, chaotic orbits and slow regular spikes (“singlet bursting”). Here we determine stability diagrams for this map, which may be thought of as a discrete-time analogous of the Hindmarsh-Rose neuron [7]. We focus exclusively on the lines at which the fixed point loses stability, which define the limit of the excitability region. We extend previous results by obtaining diagrams beyond the adiabatic limit, where the slow variable has a much slower time scale than the other two [6].

## 2 The model

The following three-dimensional non-linear map has been proposed as a minimal excitable bursting cell model [6]:

$$\begin{aligned} x(t+1) &= \tanh\left(\frac{x(t) - Ky(t) + z(t) + I(t)}{T}\right), \\ y(t+1) &= x(t), \\ z(t+1) &= (1 - \delta)z(t) - \lambda(x(t) - x_R). \end{aligned} \tag{1}$$

Like in the Hindmarsh-Rose model [7], the variable  $x$  represents the instantaneous membrane potential,  $y$  is a recovery variable and  $z$  can be considered a slow adaptive current if  $\delta$  and  $\lambda$  are set to small values ( $\ll 1$ ). Under these conditions, we can identify  $z(t)$  with e.g. the  $\text{Ca}^{2+}$ -dependent  $\text{K}^+$  current  $I_{AHP}$  [8, 9], since its time scale and general effect (long lasting hyperpolarization and adaptation of firing rates) are very similar.  $I(t)$  represents an external current which can model the effects of a synapse, a stimulus-induced ionic flow in sensory cells, or an experimentally controlled clamped current.

If we set  $z(t) = H = \text{const}$ , we are left with the fast dynamical system  $(x, y)$  which has been studied in Ref. [5]. The analysis of the two-variable system shows [5] that, with  $T$  and  $K$  fixed, a sub-critical Hopf bifurcation occurs if we increase the term  $H+I$  (that is, the bias parameter  $H$  and the external current  $I$ ). With  $I = 0$ , the autonomous behavior is controlled by the bias term  $H$  and changes dramatically at the bifurcation value  $H_c^\pm = T \operatorname{atanh}(x_c^\pm) - (1 - K)x_c^\pm$ , where  $x_c^\pm = \pm\sqrt{1 - T/K}$ .

Close to the bifurcation line, the behavior is that of an excitable cell [5]. Since the Hopf bifurcation is sub-critical (“hard excitation”), this model belongs

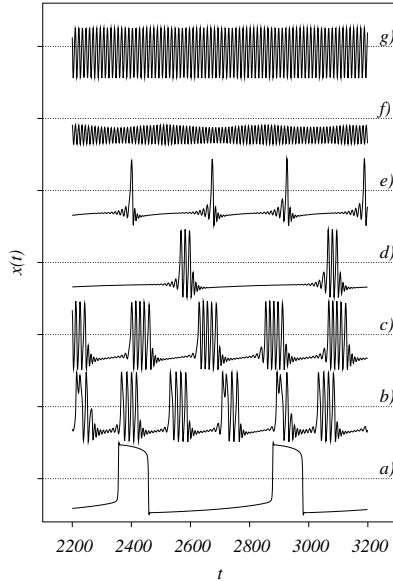


Fig. 1. Different dynamical behaviors of the three-dimensional map for  $K = 0.6$ . Unless otherwise stated,  $T = 0.35$  and  $\delta = \lambda = 0.001$ : a) cardiac-like spikes (spikes with plateau,  $T = 0.25$ ,  $x_R = -0.5$ ); b) chaotic behavior ( $T = 0.322$ ,  $x_R = -0.4$ ); bursting behavior in c) ( $x_R = -0.45$ ) and d) ( $x_R = -0.6$ ); e) regular spiking or “singlet bursting” ( $\delta = \lambda = 0.003$ ,  $x_R = -0.62$ ); f) sub-threshold oscillations ( $T = 0.45$ ,  $x_R = -0.5$ ) and g) fast spiking ( $T = 0.45$ ,  $x_R = -0.2$ ). For better visualization, the curves have been shifted vertically by 2 (dimensionless) units. The dotted lines correspond to  $x = 0$ .

to the class of the FitzHugh-Nagumo and Hodgkin-Huxley models (class I neurons) [10, 9], where the stable fixed point is a focus (perturbations lead to spiraling behavior in the phase plane). These small oscillations are described in biophysical models, after linearization about the fixed point, as a phenomenological inductance behavior (see chapter 10 in [9]).

### 3 Stability Diagrams for the Three-Dimensional Map

The three-variable model presents several qualitatively different dynamical behaviors which are usual in real biological neurons (Fig. 1). In particular, the slow current  $z(t)$  is responsible for the bursting dynamics, as discussed by Rinzel and Ermentrout [8]. This slow dynamics is controlled by the parameters  $(\delta, \lambda, x_R)$ . In what follows, we focus on the analysis of the stability diagrams in terms of these parameters. The lines where the fixed point  $(x_*, y_*, z_*)$  loses stability (for  $I = 0$ ) have been determined by standard linear stability analysis, which yields the equation

$$-\Lambda^3 + [\alpha + (1 - \delta)]\Lambda^2 - \alpha[\lambda + K + 1 - \delta]\Lambda + K\alpha(1 - \delta) = 0 \quad (2)$$

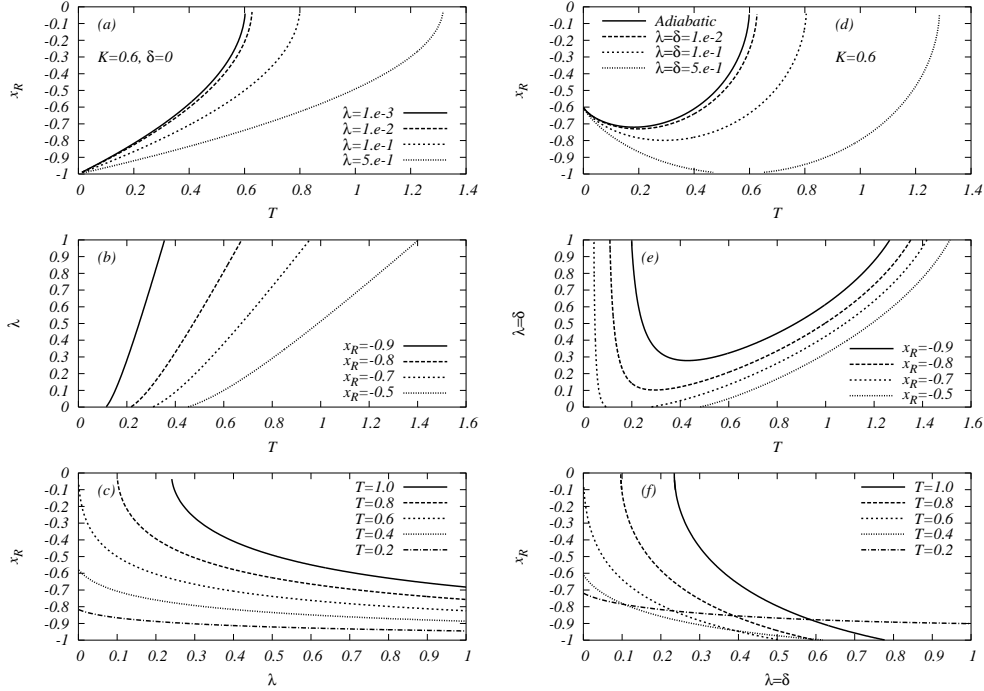


Fig. 2. Left panel: bifurcations for  $\delta = 0$ . Right panel: bifurcations for  $\lambda = \delta$ . The fixed point is stable below the lines.

for the eigenvalues  $\Lambda$ , where  $\alpha = (1 - x_*^2)/T$ .

### 3.1 The case $\delta = 0$

The case  $\delta = 0$  provides a limiting behavior where the neuron can be “perfectly adaptive”. This means that, when the fixed point is stable, adding an external current  $I$  produces a transient response: firing only occurs while  $z(t)$  is adapting (phasic firing) [6]. The fixed points can be determined exactly in that case:  $x_* = y_* = x_R$  and  $z_* = T \operatorname{atanh}(x_R) - (1 - K)x_R$ . This system presents monotonic behavior as far as loss of stability is concerned, as shown in the left panel of Fig. 2: with all the other parameters frozen, the fixed point loses stability by either increasing  $x_R$ , increasing  $\lambda$  or decreasing  $T$ .

### 3.2 The case $\lambda = \delta$

The subspace  $\lambda = \delta$  reflects the simple case where the time scales of the inflow ( $\lambda$ ) and outflow ( $\delta$ ) of the  $z$  current are the same. As opposed to the  $\delta = 0$  case, the bifurcation line in the  $x_R$  vs.  $T$  plane now presents a minimum, signaling that for sufficiently low values of  $x_R$ , the fixed point can become stable by lowering  $T$  (Fig. 2d). This non-monotonic behavior in the parameter  $T$  is also

observed in the planes  $(T, \lambda)$  and  $(\lambda, x_R)$  (Figs. 2e and 2f).

### 3.3 Adiabatic approximation

In the limit of  $\delta, \lambda \ll 1$  one can obtain analytical results by means of an adiabatic approximation. By taking  $z$  to be a quasi-static variable, in the fixed point region the stationary  $z_*$  value is determined by  $z_* = (\lambda/\delta)(x_R - x_*)$ . It is thus clear that the parameter  $x_R$  is essential for controlling the equilibrium value of  $z$ . Applying the results for the fast sub-system [5], the adiabatic approximation  $(z_*)_c = H_c$  defines a critical value for the reversion potential:  $x_R^c(T) = x_c^\pm + (\delta/\lambda)H_c^\pm = \pm [1 - (\delta/\lambda)(1 - K)] \sqrt{1 - T/K} \pm (\delta/\lambda)T \operatorname{atanh}(\sqrt{1 - T/K})$ . This critical line is plotted in the  $(x_R, T)$  plane for  $K = 0.6$  (Fig. 2d), and is visually indistinguishable from the results for  $\lambda = \delta = 0.001$ .

### 3.4 The $(I, T)$ plane

As observed in the previous section, within the adiabatic approximation the critical current  $I_c$  for the three-variable model can be readily obtained from the two-dimensional result,  $I_c = H_c - z_* = H_c(T) + (\lambda/\delta)(x_c(T) - x_R)$ , with  $H_c = \min\{H_c^+, H_c^-\}$  and  $x_c = \min\{x_c^+, x_c^-\}$ . Remembering that the critical  $x_R^c$  for  $I = 0$  is  $x_c + (\delta/\lambda)H_c$ , we finally get  $I_c(T) = (\lambda/\delta)(x_R^c(T) - x_R)$ . This means that the fixed point stability boundary  $I_c(T)$  is exactly the same as the  $x_R$  versus  $T$  diagram (Fig. 2d) with a linear shift in the  $I$  scale given by the above equation. For example, if we set  $\delta = \lambda \ll 1$  and  $x_R = -1$ , the element starts firing at  $I_c(T) = x_R^c(T) + 1$ .

### 3.5 The $(\lambda, \delta)$ plane

Relaxing the constraint  $\lambda = \delta$  and moving away from the adiabatic condition  $\lambda, \delta \ll 1$  gives rise to an interesting interplay between  $\delta$ ,  $\lambda$  and  $T$ . Fig. 3a shows the  $\delta$  vs  $\lambda$  stability boundaries for  $T = 0.34$ . While the effect of  $x_R$  remains monotonic (i.e. larger values of  $x_R$  tend to destabilize the fixed points), the curves  $\delta_c(\lambda)$  have a maximum. An interesting phenomenon occurs if  $T$  is lowered (Fig. 3b, with  $T = 0.3$ ): the shape of the boundaries changes dramatically, with larger values of  $\lambda$  inducing the instability of the fixed point. Fig. 3c shows how the curves change as  $T$  varies. For larger values of  $T$ , the stability of the system is weakly dependent on  $\lambda$ , depending rather on sufficiently small values of  $\delta$ . The change in the shapes can be intuitively understood on the

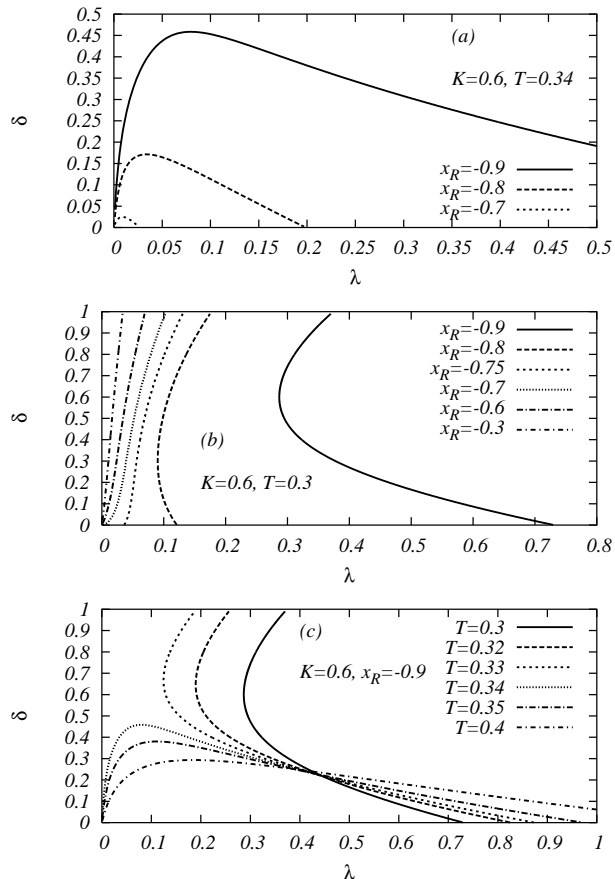


Fig. 3. Hopf bifurcations in the  $(\lambda, \delta)$  plane for  $K = 0.6$ . The fixed point is stable (a) under the lines; (b) to the left of the lines. (c) Evolution of the curves from (a) to (b).

basis of Eqs. 1: large  $T$  means small increments in the values of  $x$ , rendering the  $z$ -equation strongly dependent on  $\delta$  (Fig. 3a). For small  $T$ , on the other hand,  $\delta$  becomes less relevant: since the changes in  $x$  are larger,  $\lambda$  must be small for the fixed point to remain stable (Fig. 3b).

## 4 Conclusions

We studied a three variable nonlinear map which includes a slow dynamics over a sub-critical Hopf bifurcation generically found in class I neurons. This element is used to represent different behaviors observed in biological cells such as excitability, regular spiking, spikes with plateau and bursts [6]. We have presented bifurcation lines in different planes in the parameter space. This gives us a global understanding of the dynamics of the map and enables the proper choice of parameters for locating the excitability region. These maps can be coupled by properly modeling chemical or electrical synapses [6]. We

are currently applying this coupled map framework to large scale biologically realistic architectures, results will be published elsewhere.

## Acknowledgments

It is a pleasure to acknowledge useful discussions with A. C. Roque, J. P. Neirotti, N. Caticha, S. M. Kuva and R. F. Oliveira. We acknowledge support from CNPq, FACEPE, Projeto Enxoval-UFPE and FAPESP. We thank S. R. A. Salinas for the hospitality of the Statistical Mechanics group at IFUSP, where part of this manuscript was written.

## References

- [1] K. Aihara, T. Takabe, and M. Toyoda. Chaotic neural networks. *Phys. Lett. A*, 144:333–340, 1990.
- [2] K. Kaneko. Relevance of dynamic clustering to biological networks. *Physica D*, 75:55–73, 1994.
- [3] K. Kaneko and I. Tsuda. *Complex Systems: Chaos and Beyond, A Constructive Approach with Applications in Life Sciences*. Springer Verlag, 2000.
- [4] D. R. Chialvo. Generic excitable dynamics on a two-dimensional map. *Chaos Soliton Fract.*, 5:461–480, 1995.
- [5] O. Kinouchi and M. H. R. Tragtenberg. Modeling neurons by simple maps. *Int. J. Bifurcat. Chaos*, 6(12A):2343–3460, 1996.
- [6] S. M. Kuva, G. F. Lima, O. Kinouchi, M. H. R. Tragtenberg, and A. C. Roque. A minimal model for excitable and bursting elements. *Neurocomputing*, 38-40:255–261, 2001.
- [7] J. L. Hindmarsh and R. M. Rose. A model of neuronal bursting using three coupled first order differential equations. *Proc. Roy. Soc. London B*, 221:87–102, 1984.
- [8] J. Rinzel and B. Ermentrout. Analysis of neural excitability and oscillations. In C. Koch and I. Segev, editors, *Methods in Neuronal Modeling: From Ions to Networks*, pages 251–292. MIT Press, 2nd edition, 1998.
- [9] Christof Koch. *Biophysics of Computation*. Oxford University Press, New York, 1999.
- [10] R. FitzHugh. Thresholds and plateaus in the Hodgkin-Huxley nerve equations. *J. Gen. Physiol.*, 43:867–896, 1960.